Molecular Cell, Volume *61*

Supplemental Information

PARP1 Links CHD2-Mediated Chromatin Expansion and H3.3 Deposition to DNA Repair by Non-homologous End-Joining

Martijn S. Luijsterburg, Inge de Krijger, Wouter W. Wiegant, Rashmi G. Shah, Godelieve Smeenk, Anton J.L. de Groot, Alex Pines, Alfred C.O. Vertegaal, Jacqueline J.L. Jacobs, Girish M. Shah, and Haico van Attikum

Figure S1

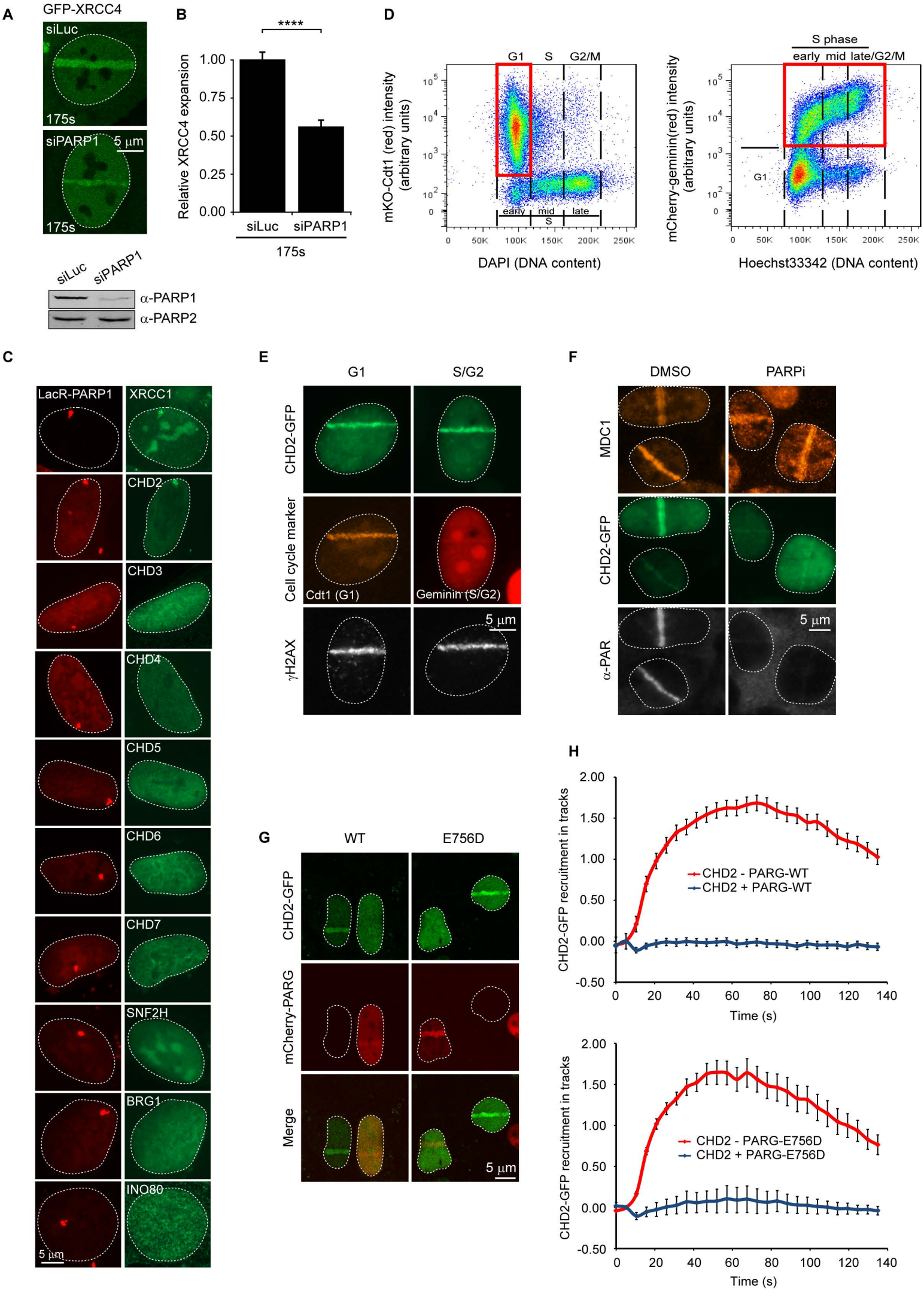
A
GFP-XRCC4
siLuc
175s
siPARP1
5 μm
175s
siLuc
siPARP1
α-PARP1
α-PARP2
B
****
Relative XRCC4 expansion
1.00
0.75
0.50
0.25
0.00
siLuc
siPARP1
175s
D
G1
S
G2/M
mKO-Cdt1 (red) intensity (arbitrary units)
early
mid
late
S
DAPI (DNA content)
S phase
early mid late/G2/M
mCherry-geminin(red) intensity (arbitrary units)
G1
Hoechst33342 (DNA content)
C
LacR-PARP1
XRCC1
CHD2
CHD3
CHD4
CHD5
CHD6
CHD7
SNF2H
BRG1
INO80
5 μm
E
G1
S/G2
CHD2-GFP
Cell cycle marker
Cdt1 (G1)
Geminin (S/G2)
γH2AX
5 μm
F
DMSO
PARPi
MDC1
CHD2-GFP
α-PAR
5 μm
G
WT
E756D
CHD2-GFP
mCherry-PARG
Merge
5 μm
H
CHD2-GFP recruitment in tracks
2.00
1.50
1.00
0.50
0.00
-0.50
0
20
40
60
80
100
120
140
Time (s)
CHD2 - PARG-WT
CHD2 + PARG-WT
CHD2 - PARG-E756D
CHD2 + PARG-E756D

Figure S1. Screen for PARP1-interacting chromatin remodelers. Related to Figure 1 and 2. (A) Expansion of GFP-XRCC4 tracks in U2OS cells transfected with PARP1 siRNAs (upper panel). Western blot showing PARP1 knockdown efficiency for the indicated siRNA (lower panel). PARP2 is a loading control. (B) Quantification of XRCC4 track expansion shown in A. 24-28 cells were analysed from 2 independent experiments. (C) U2OS 2-6-3 cells harbouring a LacO array were transfected with mCherry-LacR-PARP1 and the indicated epitope-tagged ATPases from the four major families (CHD, SWI/SNF, ISWI, INO80) of chromatin remodellers. All indicated proteins were tagged with GFP, expect for CHD3 and INO80, which were tagged with FLAG. GFP-XRCC1 is a positive control. (D) Validation of mKO-Cdt1 and mCherry-geminin cells by FACS-based cell cycle analysis. Identification of mKO-Cdt1-positive G1 and mCherry-geminin-positive S/G2 cells is shown for the respective cell lines. (E) U2OS cells expressing mKO-Cdt1 (G1 marker) or mCherry-geminin (S/G2 marker) were transfected with CHD2-GFP, UV-A micro-irradiated and stained for γH2AX. (F) U2OS cells expressing CHD2-GFP were treated with either DMSO or PARPi, micro-irradiated and stained for MDC1 and PAR chains. (G) Live cell imaging of stable CHD2-GFP cells that were transfected with mCherry-tagged PARP (WT or E756D) and subjected to multiphoton micro-irradiation. (H) Quantification of G. 20-30 cells were analysed from 2 independent experiments. Error bars represent the SEM. Statistical significance based on a two-tailed, unpaired t-test is indicated as: ****$p < 0.0001$, ***$p < 0.001$, **$p < 0.01$, *$p < 0.05$. ns, not significant.

Figure S2

A

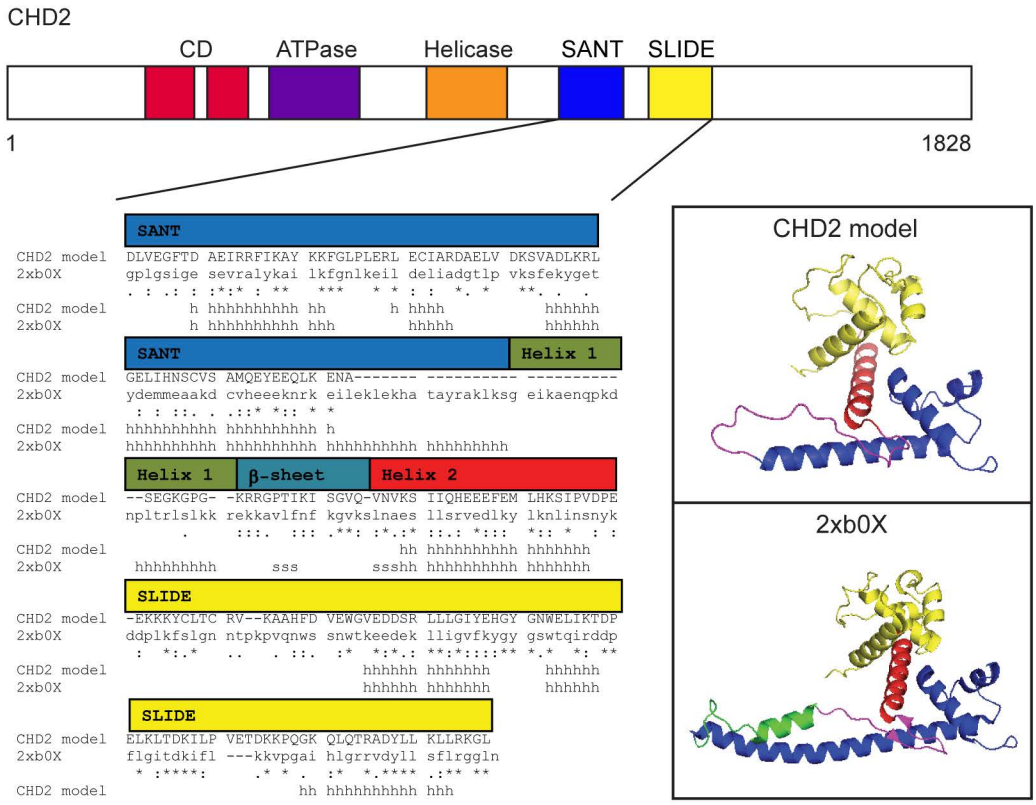

B

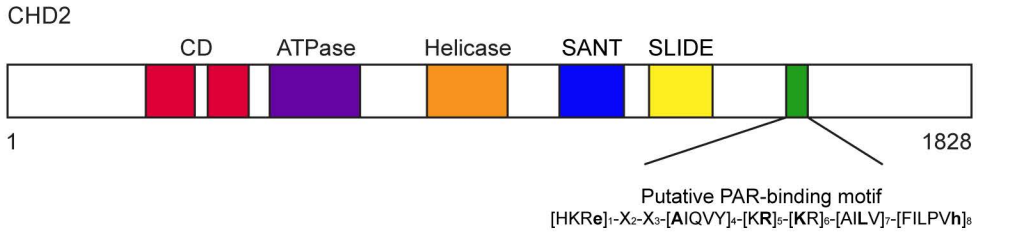

Putative PAR-binding motif
[HKRe]$_{1}$-X$_{2}$-X$_{3}$-[AIQVY]$_{4}$-[KR]$_{5}$-[KR]$_{6}$-[AILV]$_{7}$-[FILPVh]$_{8}$

CHD2_human	SKFTEFDARKLHKLYK
CHD1_human	SKFTEFDARKLHKLYK
CHD2_mouse	SKFTEFDARKLHKLYK
CHD1_chicken	SKFTEFDARKLHKLYK
CHD1_drosophila	SKFTELDAKRLFKIYK

C

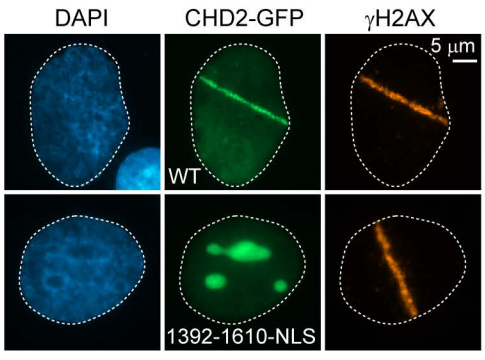

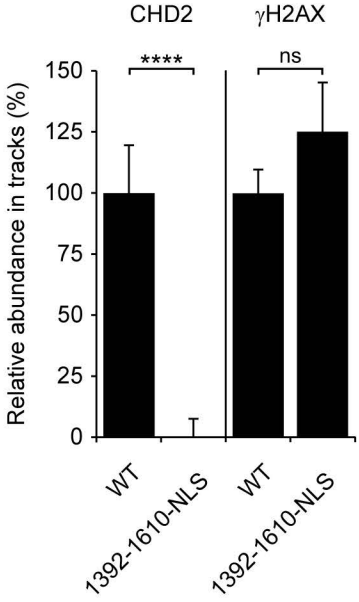

D

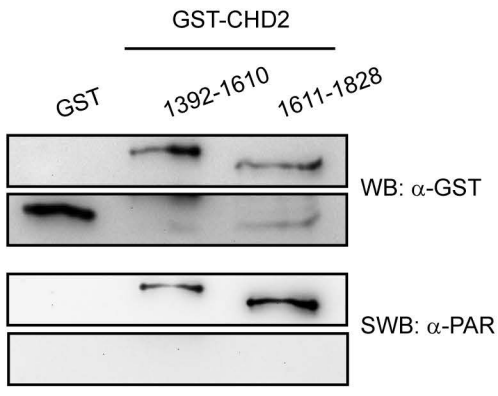

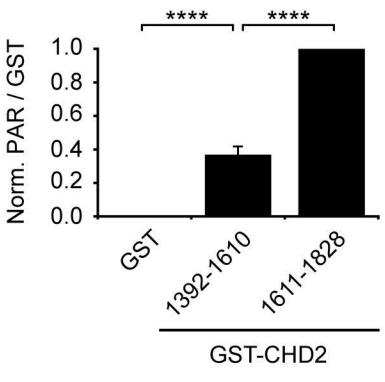

Figure S2. CHD2 contains a putative PAR-binding domain. Related to Figure 3. (A) Schematic representation of the human CHD2 protein and its domains. An amino acid sequence alignment of the putative SANT and SLIDE domains of human CHD2 and the crystallized sequence of yeast CHD1 2xb0X domain are shown (Ryan et al., 2011). Colours reflect those in the structures next to the alignment. A structural model of CHD2 SANT and SLIDE domains and the experimentally determined structure of yeast CHD1 are shown. (B) CHD2 contains a putative PAR-binding domain (green) that almost matches the consensus $[HKRe]_1$-X_2-X_3-$[AIQVY]_4$-$[KR]_5$- $[KR]_6$-$[AILV]_7$-$[FILPVh]_8$ (Gagne et al., 2008) and is conserved between human CHD1 and drosophila CHD1. (C) U2OS cells depleted for endogenous CHD2 were transfected with $CHD2^{WT}$-GFP or $CHD2^{1392\text{-}1610}$-GFP-NLS. Cells were UV-A micro-irradiated and stained for γH2AX. The quantification is shown next to the images. 22-27 cells were analysed from 2 independent experiments. (D) Association of recombinant GST-CHD2 fusion proteins with recombinant PAR was analysed by southwestern blotting. Quantification of PAR binding by the indicated CHD2 fragments. Results from three independent experiments are shown. Error bars represent the SEM. Statistical significance based on a two-tailed, unpaired t-test is indicated as: ****$p < 0.0001$, ***$p < 0.001$, **$p < 0.01$, *$p < 0.05$. ns, not significant.

Figure S3

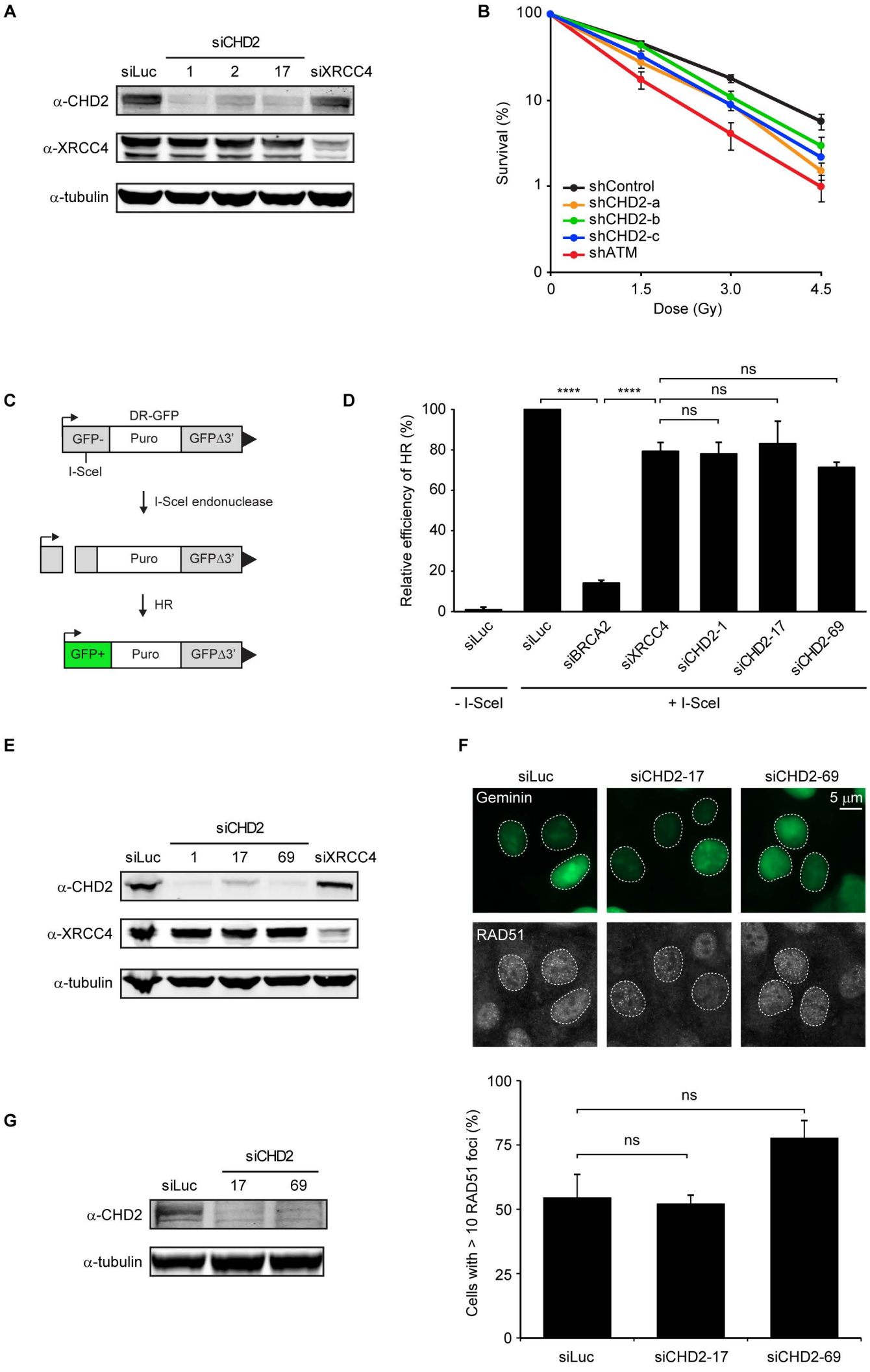
A
siCHD2
siLuc
1
2
17
siXRCC4
α-CHD2
α-XRCC4
α-tubulin
B
Survival (%)
100
10
1
0
0
1.5
3.0
4.5
Dose (Gy)
shControl
shCHD2-a
shCHD2-b
shCHD2-c
shATM
C
DR-GFP
GFP-
Puro
GFPΔ3'
I-SceI
I-SceI endonuclease
Puro
GFPΔ3'
HR
GFP+
Puro
GFPΔ3'
D
Relative efficiency of HR (%)
100
80
60
40
20
0
****
****
ns
ns
ns
siLuc
siLuc
siBRCA2
siXRCC4
siCHD2-1
siCHD2-17
siCHD2-69
- I-SceI
+ I-SceI
E
siCHD2
siLuc
1
17
69
siXRCC4
α-CHD2
α-XRCC4
α-tubulin
F
siLuc
siCHD2-17
siCHD2-69
Geminin
5 μm
RAD51
Cells with > 10 RAD51 foci (%)
100
75
50
25
0
ns
ns
siLuc
siCHD2-17
siCHD2-69
G
siCHD2
siLuc
17
69
α-CHD2
α-tubulin

Figure S3. CHD2 is not required for HR. Related to Figure 4. (A) Knock-down validation for the IR survival shown in **Fig 4A**. (B) Clonogenic survival after X-ray exposure of VH10-hTERT cells stably expressing the indicated shRNAs. (C) Schematic representation of the DR-GFP reporter for HR. (D) HEK293T cells containing the DR-GFP reporter were transfected with the indicated siRNAs and 48 hrs later co-transfected with I-SceI and mCherry expression plasmids. The percentage of GFP/mCherry-positive HEK293 cells was monitored by flow cytometry. The average of 3 experiments is shown. Error bars represent the SEM. (E) Western blot showing CHD2 and XRCC4 knockdown efficiency for the indicated siRNAs in D. (F) U2OS cells stably expressing mAG-geminin (green) were exposed to IR (10 Gy) and after 6 hrs stained for RAD51 (grey). The quantification of geminin-positive cells with more than 10 RAD51 foci is shown below the images. 100-200 cells were analysed from 2 independent experiments. Error bars represent SEM. (G) Western blot showing CHD2 knockdown efficiency for the indicated siRNAs in F. Statistical significance based on a two-tailed, unpaired t-test is indicated as: ****$p < 0.0001$, ***$p < 0.001$, **$p < 0.01$, *$p < 0.05$. ns, not significant.

Figure S4

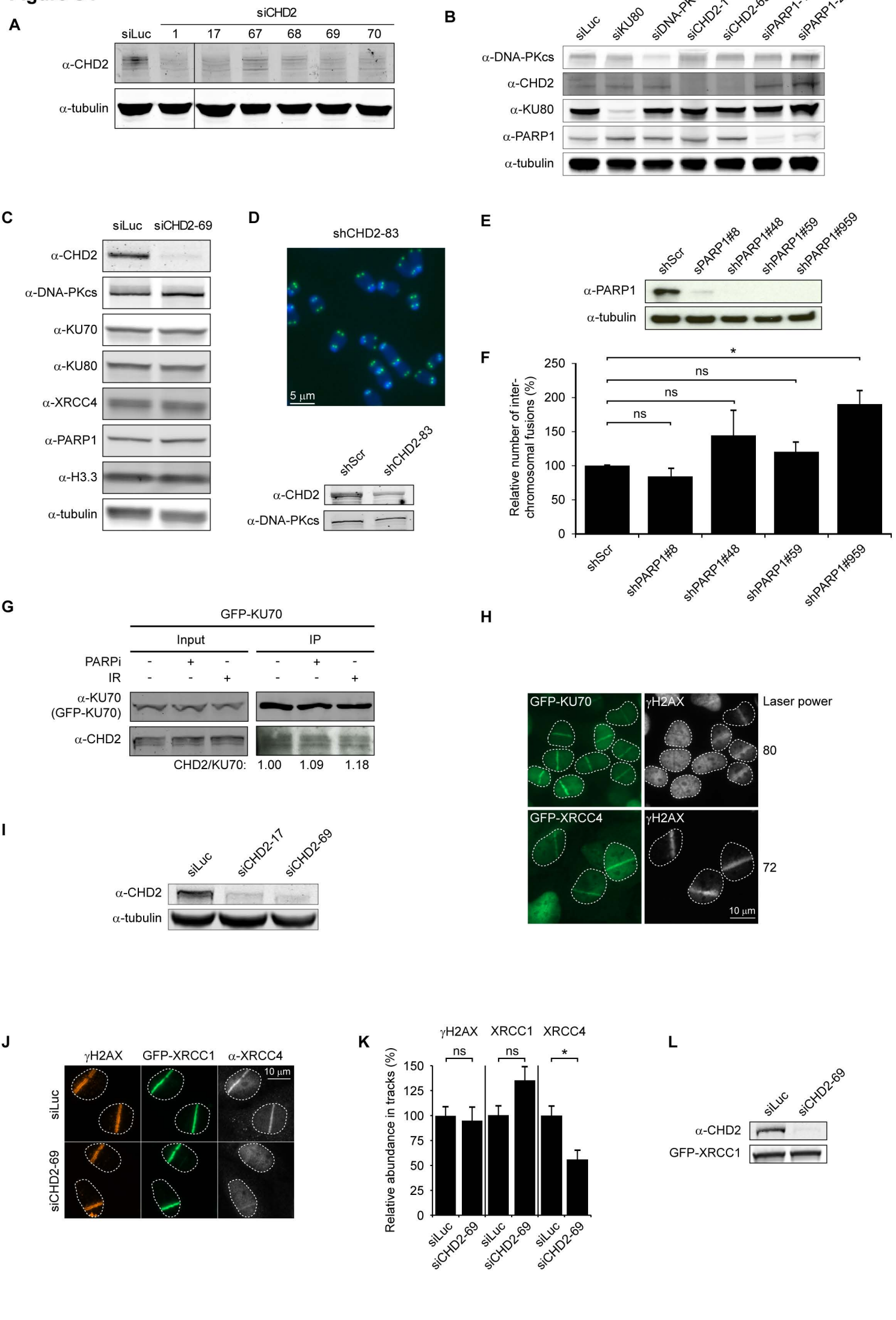
A
siCHD2
siLuc
1
17
67
68
69
70
α-CHD2
α-tubulin
B
siLuc
siKU80
siDNA-PKcs
siCHD2-1
siCHD2-69
siPARP1-1
siPARP1-2
α-DNA-PKcs
α-CHD2
α-KU80
α-PARP1
α-tubulin
C
siLuc
siCHD2-69
α-CHD2
α-DNA-PKcs
α-KU70
α-KU80
α-XRCC4
α-PARP1
α-H3.3
α-tubulin
D
shCHD2-83
5 μm
shScr
shCHD2-83
α-CHD2
α-DNA-PKcs
E
shScr
sPARP1#8
shPARP1#48
shPARP1#59
shPARP1#959
α-PARP1
α-tubulin
F
Relative number of inter-chromosomal fusions (%)
250
200
150
100
50
0
*
ns
ns
ns
shScr
shPARP1#8
shPARP1#48
shPARP1#59
shPARP1#959
G
GFP-KU70
Input
IP
PARPi
IR
α-KU70 (GFP-KU70)
α-CHD2
CHD2/KU70:
1.00
1.09
1.18
H
GFP-KU70
γH2AX
Laser power
80
GFP-XRCC4
γH2AX
72
10 μm
I
siLuc
siCHD2-17
siCHD2-69
α-CHD2
α-tubulin
J
γH2AX
GFP-XRCC1
α-XRCC4
10 μm
siLuc
siCHD2-69
K
γH2AX
XRCC1
XRCC4
Relative abundance in tracks (%)
150
125
100
75
50
25
0
ns
ns
*
siLuc
siCHD2-69
siLuc
siCHD2-69
siLuc
siCHD2-69
L
siLuc
siCHD2-69
α-CHD2
GFP-XRCC1

Figure S4. CHD2 regulates NHEJ. Related to Figure 4 and 5. (A) Western blot showing CHD2 knockdown efficiency for the indicated siRNAs in **Fig 4C**. (B) Western blot showing KU80, DNA-PKcs, CHD2 and PARP1 knockdown efficiency for the indicated siRNAs in **Fig 4E**. (C) Western blot showing that knock-down of CHD2 in U2OS cells does not affect the steady-state levels of NHEJ proteins, PARP1 or H3.3. (D) Representative image of a metaphase from TRF2^{ts} MEFs transduced with the indicated shRNA after 24hrs of telomere uncapping. Telomere-FISH shows the position of the telomeres (green), while chromosomes are stained by DAPI (blue). The western blot shows CHD2 knock-down efficiency for the indicated shRNA. The quantification is shown in **Fig. 4I**. (E) Western blot showing PARP1 knockdown efficiency for the indicated shRNAs in TRF2^{ts} MEFs. (F) Quantification of interchromosomal fusions observed in cells transduced with the indicated shRNAs. Values for cells treated with scrabled control shRNA (shScr) were set to 100%. 1600-3900 chromosomes were analysed from 2-4 independent experiments. Error bars represent the SEM. (G) Co-IP of GFP-KU70 and endogenous CHD2 in U2OS cells that were left untreated or treated with PARP inhibitor (10 μM) or exposure to IR (20 Gy). (H) Accrual of GFP-KU70 or GFP-XRCC4 to sites of UV-A micro-irradiation requires different laser power as indicated by the pan-nuclear or localized appearance of γH2AX. (I) Western blot showing CHD2 knockdown efficiency for the indicated siRNAs in **Fig 5C**. (J) U2OS GFP-XRCC1 cells were transfected with the indicated siRNAs, UV-A micro-irradiated and stained for γH2AX and XRCC4. (K) Quantification of results from J. 25-45 cells were analysed from 2 independent experiments. Error bars represent SEM. (L) Western blot showing CHD2 knockdown efficiency for the indicated siRNA in J. Statistical significance based on a two-tailed, unpaired t-test is indicated as: ****$p < 0.0001$, ***$p < 0.001$, **$p < 0.01$, *$p < 0.05$. ns, not significant.

Figure S5

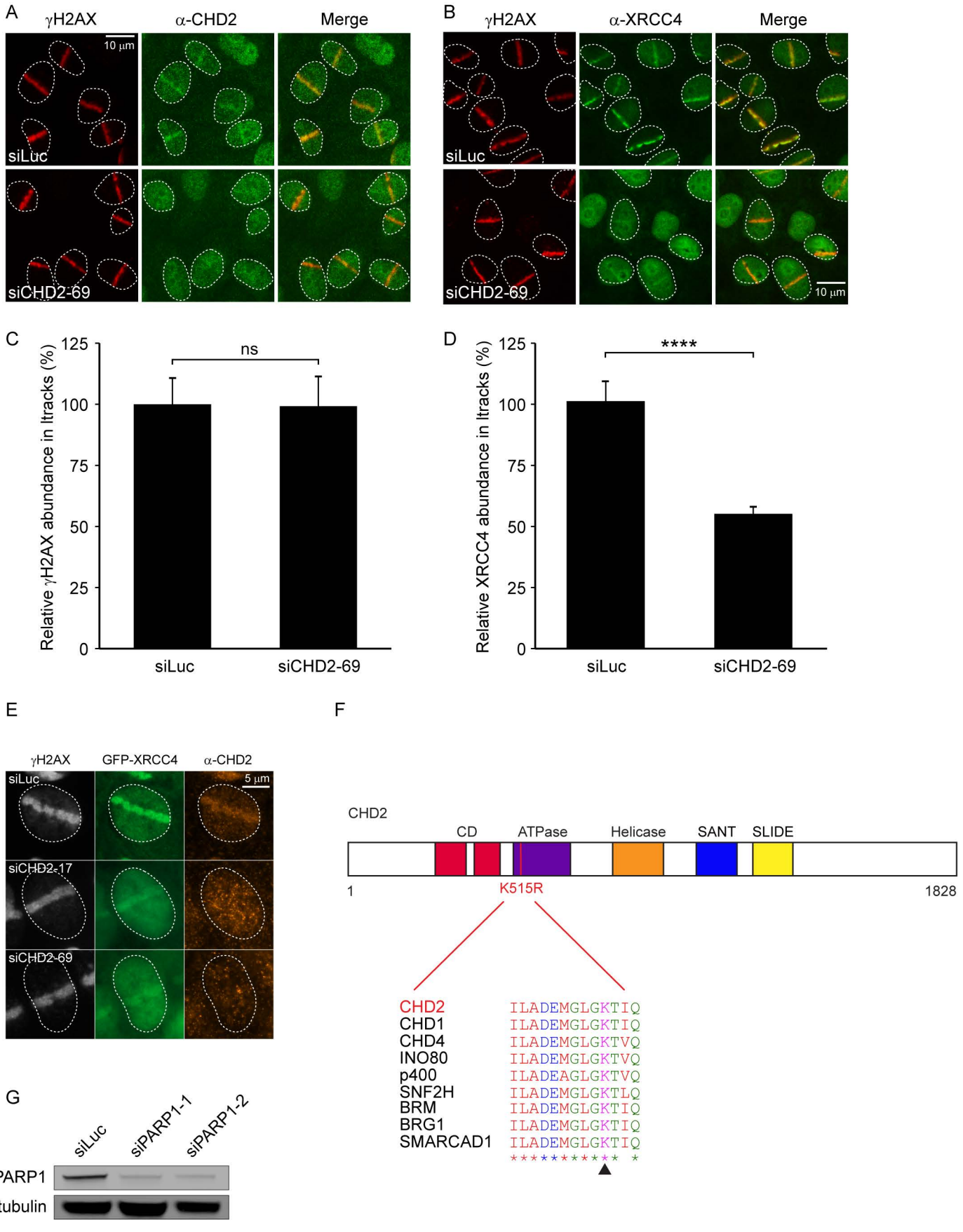
A
γH2AX
α-CHD2
Merge
10 μm
siLuc
siCHD2-69
B
γH2AX
α-XRCC4
Merge
siLuc
siCHD2-69
10 μm
C
Relative γH2AX abundance in Itracks (%)
125
100
75
50
25
0
ns
siLuc
siCHD2-69
D
Relative XRCC4 abundance in Itracks (%)
125
100
75
50
25
0
****
siLuc
siCHD2-69
E
γH2AX
GFP-XRCC4
α-CHD2
siLuc
5 μm
siCHD2-17
siCHD2-69
F
CHD2
CD
ATPase
Helicase
SANT
SLIDE
1
K515R
1828
CHD2 ILADEMGLGKTIQ
CHD1 ILADEMGLGKTIQ
CHD4 ILADEMGLGKTVQ
INO80 ILADEMGLGKTVQ
p400 ILADEAGLGKTVQ
SNF2H ILADEMGLGKTLQ
BRM ILADEMGLGKTIQ
BRG1 ILADEMGLGKTIQ
SMARCAD1 ILADEMGLGKTIQ
****
G
siLuc
siPARP1-1
siPARP1-2
α-PARP1
α-tubulin

Figure S5. CHD2 promotes recruitment of XRCC4. Related to Figure 5. (A-B) U2OS cells were transfected with the indicated siRNAs, sensitized with BrdU and UV-A micro-irradiated. Cells were fixed and stained for (A) γH2AX and CHD2, or (B) γH2AX and XRCC4. (C-D) Quantification of the results from A and B. Between 60-90 cells were analysed from 2 independent experiments. Error bars represent the SEM. (E) U2OS cells expressing GFP-XRCC4 were transfected with the indicated siRNAs, micro-irradiated and stained for γH2AX and CHD2. (F) Schematic representation of the human CHD2 protein and its domains. A region corresponding to the conserved ATP-binding pocket is aligned to that of several other human chromatin remodellers. The arrow points to the conserved lysine at position 515 that was mutated to arginine (K515R) to serve as a dominant-negative in **Fig 5E**. (G) Western blot showing PARP1 knock-down efficiency for the indicated siRNAs in **Fig 5G** and **Fig 7E**. Statistical significance based on a two-tailed, unpaired t-test is indicated as: ****$p < 0.0001$, ***$p < 0.001$, **$p < 0.01$, *$p < 0.05$. ns, not significant.

Figure S6

CHD2-GFP

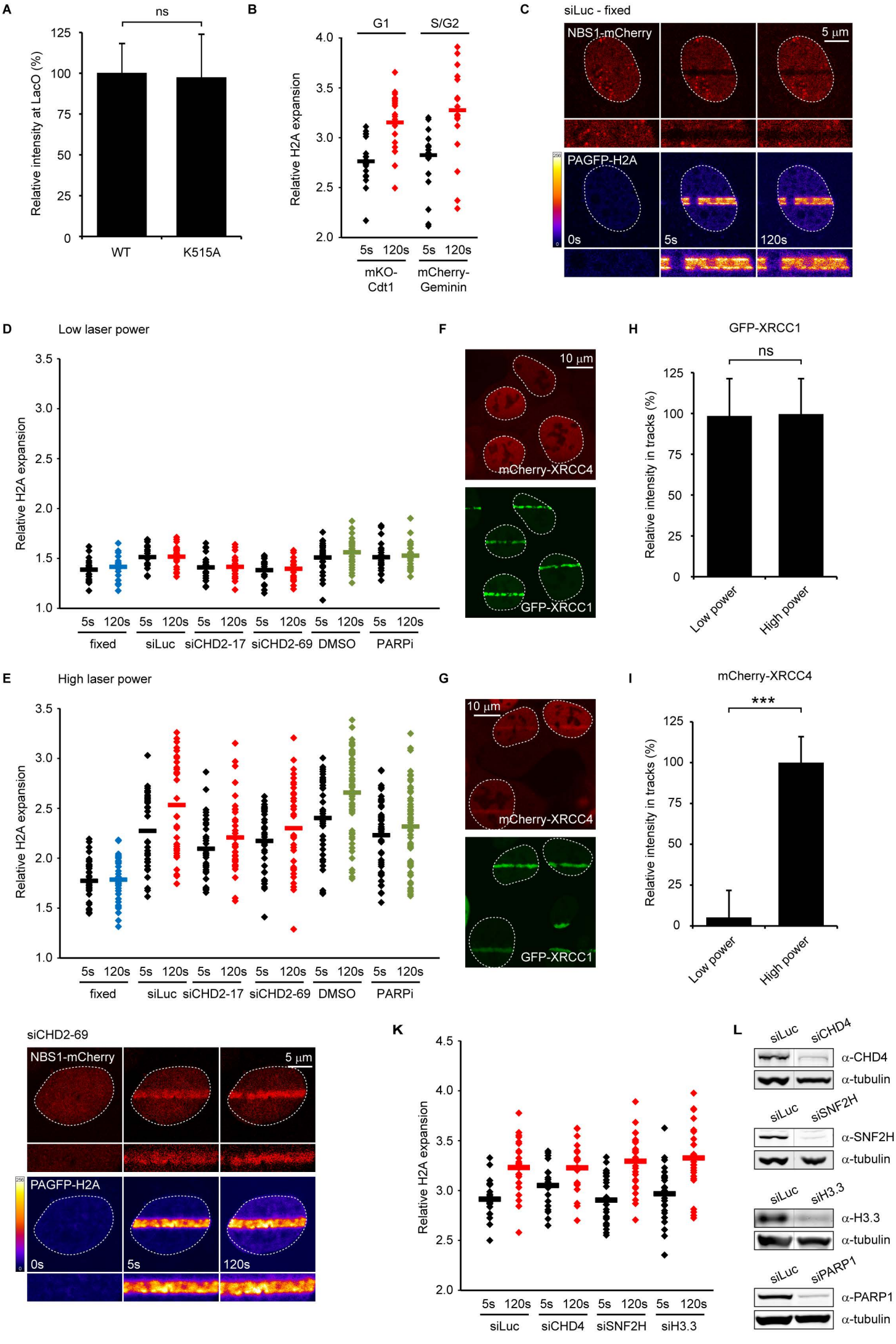

Figure S6. DNA damage-induced chromatin changes correlate with the presence of DSBs. Related to Figure 6. (A) Quantification of the recruitment of $CHD2^{WT\text{-}GFP}$ or $CHD2^{K515R}$-GFP to the LacO array upon tethering αGFP-mCherry-LacR as shown in **Fig 6A**. 33-45 cells were analysed from 2 independent experiments. (B) Chromatin expansion in U2OS cells expressing PAGFP-H2A and either mKO-Cdt1 or mCherry-geminin. Cells were micro-irradiated to simultaneously induce DNA damage and photoactivate PAGFP. 20-22 cells were analysed from 2 independent experiments. (C) Absence of expansion of PAGFP-H2A tracks in fixed U2OS cells transfected with siLuc siRNAs. Note that NBS1-mCherry is bleached and does not accumulate. (D) U2OS cells expressing PAGFP-H2A were micro-irradiated to simultaneously induce DNA damage and photoactivate PAGFP. Low laser settings were used and no appreciable chromatin changes could be detected. (E) As in D, but with higher laser settings, which triggered substantial chromatin expansion. The average of this data is shown in **Fig 6F**. (F) Stable mCherry-XRCC4 cells were co-transfected with GFP-XRCC1 followed by micro-irradiation with low laser power as in D. mCherry-XRCC4 does not accumulate under these conditions, while robust GFP-XRCC1 recruitment is detected. (G) As in F, but following micro-irradiation with higher laser settings as in E. In addition to GFP-XRCC1, also mCherry-XRCC4 is recruited under these conditions, which also trigger pronounced DNA damage-induced chromatin changes as shown in E. The extent of (H) GFP-XRCC1 and (I) mCherry-XRCC4 recruitment under these conditions is quantified. 15-20 cells were analysed from 2 independent experiments. (J) Expansion of PAGFP-H2A tracks in U2OS cells transfected with the indicated siRNA in **Fig 6F**. NBS1-mCherry was as a DNA damage marker. (K) Quantification of chromatin expansion measured by PAGFP-H2A photo-activation in cells transfected with the indicated siRNAs. 22-27 cells were analysed from 2 independent experiments. Error bars represent SEM. (L) Western blot showing CHD4, SNF2H, H3.3 and PARP1 knockdown efficiency for the indicated siRNAs in K (CHD4, SNF2H, H3.3) and **Fig 6F** (PARP1). Statistical significance based on a two-tailed, unpaired t-test is indicated as: ****$p < 0.0001$, ***$p < 0.001$, **$p < 0.01$, *$p < 0.05$. ns, not significant.

Figure S7

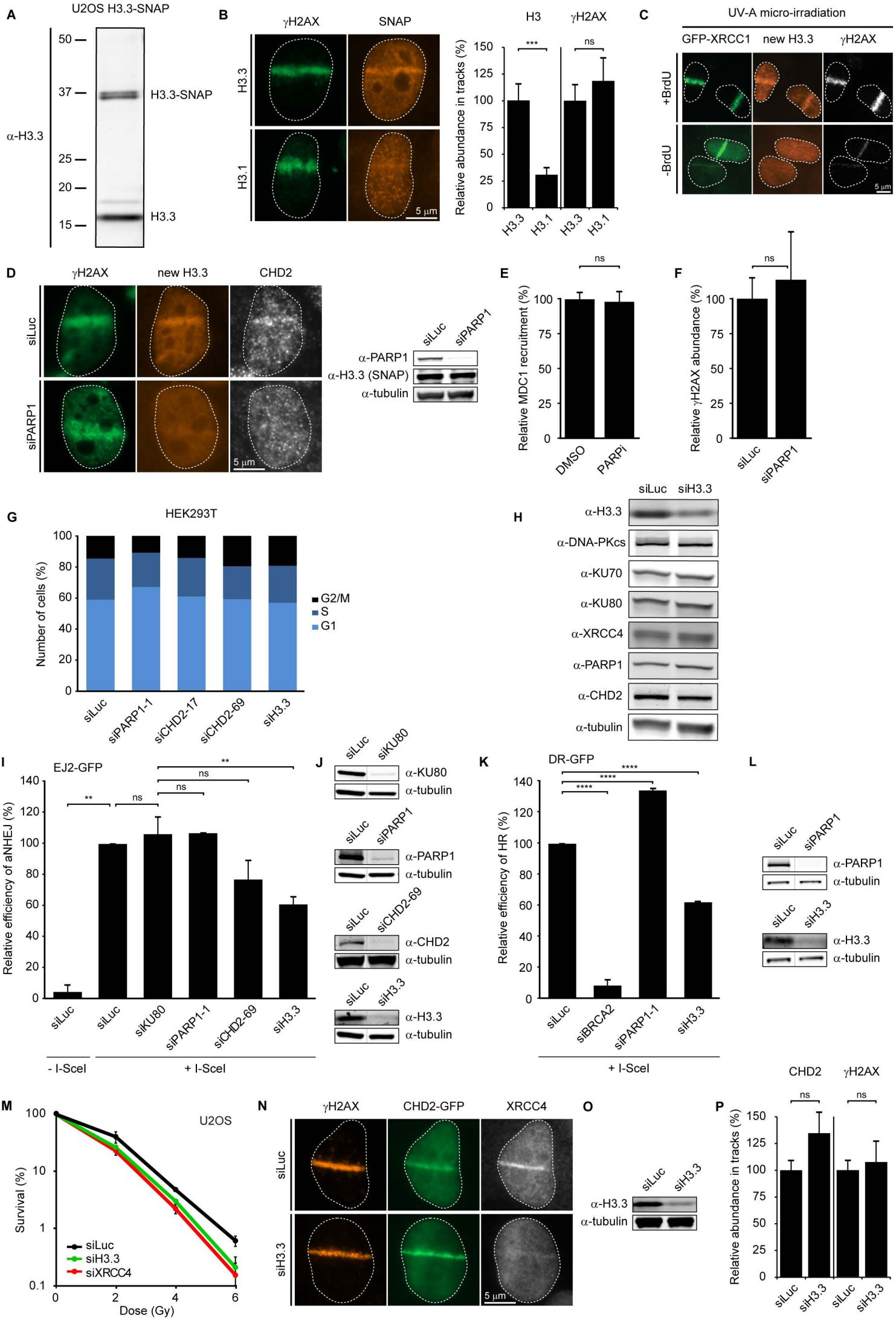
A
U2OS H3.3-SNAP
50
37
25
20
15
α-H3.3
H3.3-SNAP
H3.3
B
γH2AX
SNAP
H3.3
H3.1
5 μm
H3
γH2AX
Relative abundance in tracks (%)
***
ns
H3.3
H3.1
H3.3
H3.1
C
UV-A micro-irradiation
GFP-XRCC1
new H3.3
γH2AX
+BrdU
-BrdU
5 μm
D
γH2AX
new H3.3
CHD2
siLuc
siPARP1
5 μm
siLuc
siPARP1
α-PARP1
α-H3.3 (SNAP)
α-tubulin
E
ns
Relative MDC1 recruitment (%)
DMSO
PARPi
F
ns
Relative γH2AX abundance (%)
siLuc
siPARP1
G
HEK293T
Number of cells (%)
G2/M
S
G1
siLuc
siPARP1-1
siCHD2-17
siCHD2-69
siH3.3
H
siLuc
siH3.3
α-H3.3
α-DNA-PKcs
α-KU70
α-KU80
α-XRCC4
α-PARP1
α-CHD2
α-tubulin
I
EJ2-GFP
Relative efficiency of aNHEJ (%)
**
ns
ns
**
siLuc
siLuc
siKU80
siPARP1-1
siCHD2-69
siH3.3
- I-SceI
+ I-SceI
J
siLuc
siKU80
α-KU80
α-tubulin
siLuc
siPARP1
α-PARP1
α-tubulin
siLuc
siCHD2-69
α-CHD2
α-tubulin
siLuc
siH3.3
α-H3.3
α-tubulin
K
DR-GFP
Relative efficiency of HR (%)
****
****
****
siLuc
siBRCA2
siPARP1-1
siH3.3
+ I-SceI
L
siLuc
siPARP1
α-PARP1
α-tubulin
siLuc
siH3.3
α-H3.3
α-tubulin
M
U2OS
Survival (%)
siLuc
siH3.3
siXRCC4
Dose (Gy)
N
γH2AX
CHD2-GFP
XRCC4
siLuc
siH3.3
5 μm
O
siLuc
siH3.3
α-H3.3
α-tubulin
P
CHD2
γH2AX
ns
ns
Relative abundance in tracks (%)
siLuc
siH3.3
siLuc
siH3.3

Figure S7. H3.3 acts at DSB sites to promote DNA repair. Related to Figure 7. (A) Western blot of U2OS cells stably expressing SNAP-tagged H3.3 showing expression of endogenous H3 and H3.3-SNAP. (B) Deposition of H3.3-SNAP compared to H3.1-SNAP at sites of DNA damage 5 min after UV-A micro-irradiation (left). For quantification (right) 23-26 cells were analysed from 2 independent experiments. (C) H3.3 deposition in untreated or BrdU-sensitized cells after UV-A micro-irradiation. GFP-XRCC1 and γH2AX were included as damage markers for single-strand breaks and DSBs, respectively. (D) H3.3-SNAP deposition in cells transfected with the indicated siRNAs. Cells were also stained for γH2AX and CHD2 (left). Western blot showing PARP1 knock-down efficiency (right). The quantification of this data is shown in **Fig 7H**. (E) Quantification of the recruitment of MDC1 in H3.3-SNAP cells treated with DMSO or PARPi from **Fig 7G**. (F) Quantification of the enrichment of γH2AX in H3.3-SNAP cells transfected with siLuc or siPARP1 from **Fig 7H**. (G) Cell cycle profile of HEK293T cells transfected with the indicated siRNAs. (H) Western blot showing that knock-down of H3.3 in U2OS cells does not affect the steady-state levels of CHD2, PARP1 or NHEJ proteins. (I) U2OS cells containing the EJ2-GFP reporter for aNHEJ were transfected with the indicated siRNAs and 48 hrs later co-transfected with an I-SceI expression plasmid and mCherry. The percentage of GFP/mCherry-positive cells was monitored by flow cytometry. The average of 2 experiments is shown. (J) Western blot showing KU80, PARP1, CHD2 and H3.3 knockdown efficiency for the indicated siRNAs in H. (K) As in H, but using HEK293T cells containing the DR-GFP reporter. (L) Western blot showing PARP1 and H3.3 knockdown efficiency for the indicated siRNAs in J. (M) Clonogenic survival after X-ray exposure in U2OS cells transfected with the indicated siRNAs. (N) U2OS cells expressing CHD2-GFP were transfected with the indicated siRNAs, UV-A micro-irradiated and stained for γH2AX and XRCC4. (O) Western blot showing H3.3 knockdown efficiency for the indicated siRNA in M. (P) Quantification of the results in N. 21-31 cells were analysed from 2 independent experiments. Error bars represent the SEM. Statistical significance based on a two-tailed, unpaired t-test is indicated as: ****$p < 0.0001$, ***$p < 0.001$, **$p < 0.01$, *$p < 0.05$. ns, not significant.

Table S1. List of CHD2-GFP-interacting proteins identified by mass spectrometry. Related to Figure 1. SILAC-labelled U2OS cells expressing GFP (L) or CHD2-GFP (H) were subjected to immunoprecipition using GFP Trap beads. Following trypsin digestion and desalting, eluted peptides of the H and L precipitates were mixed in a 1:1 ratio and analysed on a Q-Exactive Orbitrap mass spectrometer. Raw MS files were analysed with the MaxQuant software suite. The H/L ratios and number of unique peptides are indicated.

Extended Experimental Procedures

Cell lines. Human HEK293, VH10-SV40, RPE-1-hTERT, Phoenix and U2OS cells were cultured at 37°C in an atmosphere of 5% CO2 in DMEM, supplemented with antibiotics, 10% fetal calf serum and glutaMAX (Gibco). U2OS 2–6-3 cells containing 200 copies of a LacO-containing cassette (~4 Mbp) were a gift from Susan Janicki (Janicki et al., 2004). U2OS 2-6-3 cells stably expressing ER-mCherry-LacR-FokI-DD (Tang et al., 2013) were induced for 5 h by 1 μM Shield-1 (Clontech) and 1 μM 4-OHT (Sigma). HEK293T cells with stably integrated DR-GFP, EJ2-GFP or EJ5-GFP reporters were gifts from Jeremy Stark and Maria Jasin (Bennardo et al., 2008; Pierce et al., 1999). HeLa cells stably expressing KU70-GFP were a gift from Dik van Gent (Mari et al., 2006). U2OS cells stably expressing GFP-XRCC1 were a gift from Niels Mailand (Bekker-Jensen et al., 2007). U2OS cells stably expressing H3.1-SNAP were a gift from Sophie Polo (Adam et al., 2013). U2OS cells stably expressing GFP/mCherry-XRCC4, CHD2-GFP or H3.3-SNAP were generated by transfection and selection with puromycin (1 μg/ml) or G418 (400 μg/ml), respectively. U2OS cells stably expressing cell cycle markers mKO-Cdt1, mCherry-geminin or mAG-geminin were generated by lentiviral infection. VH10-hTERT cells stably expressing shRNAs (see list of shRNA sequences) were generated using retroviral infection. *Trf2*$^{-/-}$*;p53*$^{-/-}$*;*TRF2^{ts} MEFs harboring the temperature-sensitive TRF2^{I468A} (TRF2^{ts}) allele were generated from *Trf2*$^{flox/-}$ *p53*$^{-/-}$ MEFs as described previously (Konishi and de Lange, 2008; Peuscher and Jacobs, 2011). TRF2ts MEFs were maintained at the permissive temperature of 32 °C and only grown at 39 °C to induce telomere uncapping through inactivation of TRF2.

Chemicals. PARP inhibitor (KU-0058948) was a gift from Mark O'Connor (Astrazeneca) and used at a concentration of 1-10 μM.

Plasmids. The full-length human CHD2 cDNA (5.5 kb) was amplified by PCR from plasmid pCMV6-XL4-CHD2 (Open Biosystems) and inserted into pEGFP-N1 (Clontech). All indicated deletion mutants or point mutants of CHD2 were generated by PCR and cloning (see list of primers). siRNA-resistant CHD2 was generated by introducing the underlined mutations: GA<u>A</u>GG<u>G</u>AA<u>G</u>GG<u>G</u>CC<u>C</u>GG<u>A</u>AA<u>G</u>. The CHD2 Fragment 1392-1610 was inserted into GFP-NLS to ensure nuclear localization. The CHD2$^{1392-1610}$ and CHD2$^{1611-1828}$ cDNA fragments were inserted into pDEST15 in-frame with the GST-coding sequence. A collection of cDNAs encoding various chromatin remodelers was fused in-frame with either GFP in pEGFP-C1 (Clontech) (CHD4, CHD5, CHD6, CHD7, SNF2H, BRG1) or FLAG in pCDNA3.1 (Invitrogen) (CHD3, INO80). The H3F3B gene was fused in frame with GFP or a SNAP tag (New England Biolabs). pPAGFP-H2A was generated by replacing GFP with PAGFP in the previously described vector pGFP-H2A (Luijsterburg et al., 2012b). The VHH anti-GFP gene (Herce et al., 2013) (a gift of Heinrich Leonardt) was fused in-frame to mCherry-LacR. Lentiviral plamids encoding mKO-Cdt1, mCherry-geminin and mAG-geminin were kind gifts of Atsushi Miyawaki. The XRCC4 cDNA (a gift of Penny Jeggo) was inserted into EGFP-C3-ires-puro. GFP-C3-PARP1 was a gift of Valerie

Schreiber (Mortusewicz et al., 2007). The PARP1 cDNA was inserted into mCherry-LacR-C3. Vectors encoding mCherry-PARG^{wt} or mCherry-PARG^{E756D} were gift of Michael Hendzel (Ismail et al., 2012).

Transfections. Cells were transfected with plasmid DNA using Lipofectamine 2000 according to the manufacturer's instructions. Cells were typically imaged 24 hrs after transfection. All siRNA transfections (see list of siRNA sequences) were performed with 40 or 80 nM siRNA duplexes using Lipofectamine RNAiMAX (Invitrogen). Cells were transfected twice with siRNAs at 0 and 36 hrs and were typically analyzed 60 hrs after the first transfection.

Western blotting. Cell extracts were generated by cell lysis and boiled in sample buffer. Proteins were separated by sodium dodecyl sulfate polyacrylamide gel electrophoresis (SDS-PAGE) and transferred to nitrocellulose membranes. Protein expression was analyzed by immunoblotting with the indicated primary antibodies (see list of antibodies) and secondary CF680 Goat Anti-Rabbit IgG antibodies at 1:10.000, CF770 Goat Anti-Mouse IgG antibodies at 1:5000 and CF770 Goat Anti-Rat IgG antibodies at 1:10.000 (Biotium), and detection using the Odyssey infrared imaging scanning system (LI-COR biosciences, Lincoln, Nebraska USA) or ECL.

Generation of DSBs. IR was delivered by a YXlon X-ray generator (YXlon International, 200 KV, 4 mA, dose rate 1.1 Gy/min).

Cell survival assay. VH10-SV40 or U2OS cells were transfected for 48 h with siRNA. Alternatively, VH10-hTERT cells stably expressing shRNAs were used. Cells were trypsinized, seeded at low density and exposed to IR. After 7 days, the cells were washed with 0.9% NaCl and stained with methylene blue. Colonies of more than 20 cells were scored.

Immunoprecipitation for Co-IP. HEK293 cells were transfected with plasmids encoding GFP-PARP1 or CHD2-GFP. For endogenous IPs, the relevant antibody (or corresponding IgG control) was conjugated to Protein A-coupled agarose beads (Millipore 16-157). For immunoprecipitation, cells were lysed in EBC-150 buffer (50 mM Tris, pH 7.5, 150 mM NaCl, 0.5% NP-40, 1 mM EDTA) supplemented with protease and phosphatase inhibitor cocktails. The lysed cell suspension was sonicated 6 times for 10s on ice and subsequently incubated with 500 U Benzonase for 1 hr under rotation. The NaCl concentration was increased to 300 mM and the suspension was rotated for 20 min. The cleared lysates were subjected to GFP immunoprecipitation with GFP Trap beads (Chromotek) or PARP1/CHD2/KU70 immunoprecipitation with a specific antibody. The beads were then washed 4-6 times with EBC-300 buffer (50 mM Tris, pH 7.5, 300 mM NaCl, 0.5% NP-40, 1 mM EDTA) and boiled in sample buffer. For denaturing IPs, the beads were subsequently washed twice with EBC-1000 buffer (50 mM Tris, pH 7.5, 1 M NaCl, 0.5% NP-40, 1 mM EDTA). Bound proteins were resolved by SDS-PAGE and immunoblotted with the indicated antibodies.

Generation of mass spectrometry samples. For stable isotope labeling by amino acids in cell culture (SILAC) labeling, U2OS cells were cultured for 14 days in media containing 'heavy' (H) and 'light' (L) labeled forms of the amino acids arginine and lysine respectively. SILAC-labeled cells were transiently transfected with CHD2-GFP (H) or empty vector (L) and equal amounts of H- and L-labelled cells were lysed in EBC buffer as described above. CHD2-GFP (H) or empty vector control (L) lysates were subjected to immunoprecipition using GFP Trap beads as described above. The beads were subsequently washed 2 times with EBC-300 buffer and 2 times with 50 mM $(NH_4)_2CO_3$ followed by overnight digestion using 2.5 μg trypsin at 37°C under constant shaking. Peptides of the H and L precipitates were mixed in a 1:1 ratio and desalted using a Sep-Pak tC18 cartridge by washing with 0.1 % acetic acid. Finally, peptides were eluted with 0.1 % acetic acid/60 % acetonitrile and lyophilized.

Mass spectrometry. Mass spectrometry was performed essentially as previously described (Schimmel et al., 2014). Samples were analyzed on a Q-Exactive Orbitrap mass spectrometer (Thermo Scientific, Germany) coupled to an EASY-nanoLC 1000 system (Proxeon, Odense, Denmark). Digested peptides were separated using a 13 cm fused silica capillary (ID: 75 µm, OD: 375 µm, Polymicro Technologies, California, US) in-house packed with 1.8 µm C18 beads (Reprospher-DE, Pur, Dr. Maisch, Ammerburch-Entringen, Germany). Peptides were separated by liquid chromatography using a gradient from 2% to 95% acetonitrile with 0.1% formic acid at a flow rate of 200 nl/min for 2 hrs. The mass spectrometer was operated in positive-ion mode at 2.2 kV with the capillary heated to 200°C. Data-dependent acquisition mode was used to automatically switch between full scan MS and MS/MS scans, employing a top 10 method. Full scan MS spectra were obtained with a resolution of 70,000, a target value of $3x10^6$ and a scan range from 400 to 2,000 m/z. Higher-Collisional Dissociation (HCD) tandem mass spectra (MS/MS) were recorded with a resolution of 17,500, a target value of $1x10^5$ and a normalized collision energy of 25%. The precursor ion masses selected for MS/MS analysis were subsequently dynamically excluded from MS/MS analysis for 60 sec. Precursor ions with a charge state of 1 and greater than 6 were excluded from triggering MS/MS events. Raw MS files were analysed with the MaxQuant software suite (version 1.4.1.2; Max Planck Institute of Biochemistry).

Immunoprecipitation for PAR binding assays. HEK293 cells were transfected with plasmids encoding CHD2-GFP variants. For immunoprecipitation, cell were washed and collected by scraping in cold PBS and lysed on ice for 20 min in IP-300 buffer (50 mM Tris-HCl, 5 mM EDTA, 0.2 % NP-40, 300 mM NaCl, 0.5 mM PMSF) supplemented with protease inhibitors. Lysates were subsequently sonicated for 20 sec. An equal volume of IP-300 buffer without NaCl was added and the extracts were centrifuged at maximum speed at 4°C for 10 min. The supernatant was collected in a new tube and the chromatin pellet suspended in buffer containing 20 mM Tris-HCl pH 7.5, 100 mM KCl, 2 mM MgCl2, 1 mM CaCl2, 0.3 M sucrose, 0.1 % Triton X-100, protease inhibitor, phosphatase inhibitor and PMSF. The chromatin suspension was incubated with 800 U/ml MNase at room temperature for 30 min. MNase was stopped by addition of 5 mM EDTA and EGTA followed by microcentrifugation at

maximum speed for 10 min at 4°C. The chromatin extract was combined with the collected supernatant and GFP immunoprecipitation was carried out for 12-15 hr at 4°C on a rotating stand using GFP trap beads (Chromotek). The beads were then washed five times with 50 volumes of Tris-buffered saline and 0.1 % tween (TBS-T) containing protease inhibitors and boiled for 10 min in Laemmli buffer.

Radioactive PAR synthesis. Radioactive PAR was synthesized as described earlier (Shah et al., 2011). Purified bovine PARP (6 U) was activated in 900 µl buffer containing 100 mM Tris-HCl pH 8.0, 10 mM $MgCl_2$, 10% glycerol, 10 mM DTT, 500 µM cold NAD, 250 µCi of 32P-NAD (adenylate-32P, 350 nM), 10 % ethanol and 23 µg activated calf thymus DNA. A 5 µl aliquot was retrieved to determine the initial counts per minute (cpm) in the mixture. The reaction was carried out at 30 °C for 30 min, followed by precipitation of auto-modified PARP1 on ice for 30 min, by adding 100 µl of 3 M Na-acetate pH 5.2 and 700 µl of isopropanol. The precipitated PARP1 was collected by spinning the tube at 13,000 rpm for 10 min at 4°C, washed two times with ethanol to remove the un-reacted NAD and air dried. The pellet was dissolved in 1 ml of 1 M KOH-50 mM EDTA, by heating at 60 °C for 1 hr to separate the PAR polymer from PARP1 and solubilize it. Subsequently, 9 ml of buffer AAGE9 (250 mM NH_4OAc, 6 M guanidine-HCl, 10 mM EDTA) was added and the pH was adjusted to 9. The mixture was loaded on 1 ml of DHBB resin in Econocolumns (BioRad), which was first equilibrated in 5 ml of water and 10 ml of AAGE9. The resin was washed with 20 ml of AAGE9 and 10 ml of NH_4-acetate (pH 9.0). The PAR polymer was eluted with 1 x 0.5 ml followed by 4 x 1 ml of water at 37 °C. Elutions were collected in separate Eppendorf tubes and counted on a β-counter. The concentration of PAR polymer was calculated based on the initial cpm (1 µl represents cpm/ 500 pmoles of NAD). Most radiolabelled PAR polymer was in the second elution, which was aliquoted and stored at -30 °C in a lead container.

Purification of GST-CHD2 fragments. GST-CHD2$^{1392-1610}$ and GST-CHD2$^{1611-1828}$ expression plasmids were transformed into BL21 cells, which were grown until the cells reached an OD600 of 0.6-0.8 absorbance units. To induce expression of the GST fusion proteins, 1 mM IPTG was added and cells were incubated for 4 hrs at 30 °C. After centrifugation, bacterial pellets were lysed at room temperature for 30 minutes in 2.5 ml lysis buffer (125 mM Tris, 150 mM NaCl, 1 mM $MgCl_2$ pH8, 0.1 volume BugBuster 10x, 2500 units rLysozyme, 62.5 units benzonase (Novagen-Merck), Protease Inhibitor Cocktail EDTA-free (Sigma-Aldrich)). Lysates were filtered through 0.2 µm filter membranes and incubated at room temperature for 1 hr with 500 µl Glutathione Superflow Agarose beads (Life Technologies). After binding, the Agarose beads were packed in a column and loaded on an ÅKTA chromatography system (GE Healthcare Biosciences). Columns were washed with Wash Buffer (WB; 125 mM Tris, 150 mM NaCl, pH8) and GST fusion proteins were eluted in WB containing 10 mM reduced glutathione (Sigma-Aldrich). Fractions with purified protein were collected and concentrated using Vivaspin ultrafiltration cups (Sartorius). Following concentration, the purified proteins were dissolved in 125 mM Tris, 150 mM NaCl, pH8, 10% glycerol. Purified proteins were frozen in liquid nitrogen and stored at -80 °C.

Southwestern blotting to monitor PAR and PARP1 binding. Immunoprecipitated CHD2-GFP proteins or recombinant GST-CHD2 proteins were separated in 8% SDS-PAGE denaturing gels. Purified human PARP1 was included as a positive control. Gels were incubated for 1 hr with gentle agitation in 20-30 ml of running buffer containing 5 % ß-mercaptoethanol. Proteins were then transferred to nitrocellulose membranes overnight at 35 V in a cold room. The membranes were rinsed three times in TST buffer (10 mM Tris 7.5, 150 mM NaCl, 0.05 % Tween) and incubated on a shaker at room temperature for 1 hr in the same buffer containing 250 nM radioactive PAR polymer. For CHD2-GFP studies, membranes were washed 3 times for 10 min with TST buffer, followed by 3 washes of 15 min each with the same buffer but containing 500 mM NaCl. The membranes were rinsed in the regular TST, dried and either exposed to a film or phosphoimager screen to detect radioactivity. Following the radioactive detection, membranes were blocked in PBS-MT (PBS with 5 % milk and 0.1 % tween), and probed for PARP1 followed by re-probing for GFP (see list of antibodies). For GST-CHD2 studies, membranes were washed 3 times for 10 min with TST buffer, followed by 3 washes of 10 min each with the same buffer but containing 500 mM NaCl. Membrane were rinsed with regular TST buffer, blocked in PBS-MT (PBS with 5 % milk and 0.1 % tween), and probed for PAR (10H) followed by re-probing for GST and PARP1 (see list of antibodies).

Immunofluorescent labelling. Cells were either directly fixed or pre-extracted with 0.25% Triton-X100 (Serva) in cytoskeletal (CSK) buffer (10 mM Hepes-KOH, 300 mM Sucrose, 100 mM NaCl, 3 mM $MgCl_{2,}$ pH 7.4) on ice for 2 min and subsequently fixed with 4% formaldehyde in PBS for 15 min at 4°C. Cells were post-extracted with 0.5% Triton-X100 (Serva) in PBS, and treated with 100 mM glycine in PBS for 10 min to block unreacted aldehyde groups. Cells were rinsed with phosphate-buffered saline and equilibrated in WB (PBS containing 0.5% BSA, and 0.05% Tween 20; Sigma-Aldrich). Antibody steps and washes were in WB. The primary antibodies (see list of antibodies) were incubated overnight at 4°C. Detection was done using goat anti-mouse or goat anti-rabbit Ig coupled to Alexa 488, 546 or 647 (1:1000; Invitrogen Molecular probes). Samples were incubated with 0.1 µg/ml DAPI and mounted in Polymount.

Microscopic analysis of fixed cells. Images of fixed samples were acquired on a Zeiss AxioImager M2 or D2 widefield fluorescence microscope equipped with 40x, 63x and 100x PLAN APO (1.4 NA) oil-immersion objectives (Zeiss) and an HXP 120 metal-halide lamp used for excitation. Fluorescent probes were detected using the following filters: DAPI (excitation filter: 350/50 nm, dichroic mirror: 400 nm, emission filter: 460/50 nm), GFP/Alexa 488 (excitation filter: 470/40 nm, dichroic mirror: 495 nm, emission filter: 525/50 nm), mCherry (excitation filter: 560/40 nm, dichroic mirror: 585 nm, emission filter: 630/75 nm), Alexa 555 (excitation filter: 545/25 nm, dichroic mirror: 565 nm, emission filter: 605/70 nm), Alexa 647 (excitation filter: 640/30 nm, dichroic mirror: 660 nm, emission filter: 690/50 nm). Images were recorded using ZEN 2012 software and analyzed in Image J.

Multiphoton laser micro-irradiation. U2OS cells grown on 18 mm coverslips were placed in a Chamlide CMB magnetic chamber and the growth medium was replaced by CO_2-independent

Leibovitz's L15 medium supplemented with 10% FCS and penicillin-streptomycin. Laser micro-irradiation was carried out on a Leica SP5 confocal microscope equipped with an environmental chamber set to 37°C. DSB-containing tracks (1.5 µm width) were generated with a Mira modelocked titanium-sapphire (Ti:Sapphire) laser (l = 800 nm, pulse length = 200 fs, repetition rate = 76 MHz, output power = 80 mW) using a UV-transmitting 63× 1.4 NA oil immersion objective (HCX PL APO; Leica). Confocal images were recorded before and after laser irradiation at 5 or 10 sec time intervals over a period of 2-3 min. PA–GFP-H2A was photo-activated using the same laser and settings as those used to inflict localized DNA damage.

UV-A laser micro-irradiation. U2OS cells were grown on 18 mm coverslips and sensitized with 10 µM 5′-bromo-2-deoxyuridine (BrdU) for 24 hrs as described (Acs et al., 2011; Luijsterburg et al., 2012a). For micro-irradiation, the cells were placed in a Chamlide TC-A live-cell imaging chamber that was mounted on the stage of a Leica DM IRBE widefield microscope stand (Leica) integrated with a pulsed nitrogen laser (Micropoint Ablation Laser System; Andor). The pulsed nitrogen laser (16 Hz, 364 nm) was directly coupled to the epifluorescence path of the microscope and focused through a Leica 40x HCX PLAN APO 1.25-0.75 oil-immersion objective. The growth medium was replaced by CO_2-independent Leibovitz's L15 medium supplemented with 10% FCS and penicillin-streptomycin and cells were kept at 37°C. The laser output power was set to 72 to generate strictly localized sub-nuclear DNA damage. Following micro-irradiation, cells were incubated for the indicated time-points at 37°C in Leibovitz's L15 and subsequently fixed with 4% formaldehyde before immunostaining. Typically, an average of 50 cells was micro-irradiated (2 iterations per pixel) within 10–15 min using Andor IQ software (Andor).

H3.3-SNAP labeling. U2OS cells stably expressing H3.3-SNAP were incubated with 10 µM SNAP-cell Block (New England Biolabs) in DMEM (10% FCS) for 30 min to quench pre-existing histones. Cells were incubated in fresh medium for 1.5 hrs to allow the synthesis of new H3.3 molecules and subsequently subjected to UV-A micro-irradiation. Following irradiation, newly synthesized H3.3-SNAP molecules were labeled with 2 µM SNAP-cell TMR star (New England Biolabs) in Leibovitz's L15 (10% FCS) for 15 min (pulse) after which cells were pre-extracted with 0.25% Triton-X100 (Serva, Heidelberg, Germany) in cytoskeletal (CSK) buffer (10 mM Hepes-KOH, 300 mM Sucrose, 100 mM NaCl, 3 mM MgCl2, pH 7.4) for 2 min and subsequently fixed with 4% formaldehyde.

Microscopic analysis of living cells. Images recorded after multi-photon micro-irradiation of living cells were analyzed using LAS-AF software (Leica). The average pixel intensity of laser tracks was measured within the locally irradiated area (I_{damage}), in the nucleoplasm outside the locally irradiated area ($I_{nucleoplasm}$) and in a region not containing cells in the same field of view ($I_{background}$). The relative level of accumulation expressed relative to the protein level in the nucleoplasm was calculated as follows: $((I_{damage} - I_{background})/(I_{nucleoplasm} - I_{background}) - 1)$. Track width was measured using ImageJ software.

Homologous Recombination (HR) and Non-Homologous End-Joining (NHEJ) reporter assays

HEK293 cell lines containing either a stably integrated copy of the DR-GFP, EJ5-GFP or EJ2-GFP reporter were used to measure the repair of I-S*ce*I-induced DSBs by HR or NHEJ (Bennardo et al., 2008; Pierce et al., 1999). Briefly, 48 h after siRNA transfection, cells were co-transfected with an mCherry expression vector and the I-SceI expression vector pCBASce (Pierce et al., 1999). 48 h later the percentage of GFP-positive cells among mCherry-positive cells was determined by FACS on a BD LSRII flow cytometer (BD Bioscience) using FACSDiva software version 5.0.3. Quantifications were performed using WinMDI 2.9 (freeware), FACSDiva™ (BD Biosciences) or FlowJo software (FlowJo).

Random plasmid integration assay

U2OS cells were seeded (day 1) and transfected with siRNAs in a 6 cm dish the following day (day 2). Later that day, the cells were transfected with 2 µg gel-purified BamHI-EcoRI-linearized pEGFP-C1 plasmid. The cells were subsequently transfected twice with siRNAs at 24 hrs and 36 hrs after the first transfection (day 3 and day 4, respectively). On day 5, cells were collected, counted and seeded in 15 cm dishes either lacking or containing 0.5 mg/mL G418. The transfection efficiency was determined on the same day by FACS analysis. The cells were incubated at 37°C to allow colony formation and medium was refreshed on day 8 and 12. On day 15, the cells were washed with 0.9% NaCl and stained with methylene blue. Colonies of more than 50 cells were scored. Random plasmid integration events on the G418-containing plates were normalized to the plating efficiency (plate without G418) and transfection efficiency based on GFP expression.

Chromosome fusions at uncapped telomeres assay

TRF2^{ts} MEFs were transduced with pLKO-puro shRNA lentiviruses obtained from Mission library clones (Sigma) containing shRNAs that target mouse *CHD2, PARP1, H3.3, LIGIV* or a scrambled control shRNA (see list of shRNA sequences). A retroviral shRNA and corresponding control shRNA was used for the knockdown of *LigaseIV* (Peuscher and Jacobs, 2011). Lentivirus and retrovirus production and transduction were performed as before (Peuscher and Jacobs, 2011). Following transduction, cells were selected on 4 µg/mL puromycin for 2-5 days. TRF2^{ts} MEFs infected with shRNAs constructs were shifted to the non-permissive temperature (39°C) for 24 hours to induce telomere uncapping. After 24 hrs of uncapping, cells were subjected to colcemide (Gibco) treatment for 2 hrs to enrich for metaphases. Cells were subsequently harvested by trypsinization, incubated for 7 min at 37°C in 75 µM KCl, and fixed in freshly prepared methanol:acidic acid (3:1). Cells were dropped onto wet slides and air-dried prior to hybridization (Boersma et al., 2015). Telomere-FISH was carried out by overnight hybridization with a TelC-FAM PNA probe. After hybridization, slides were washed and mounted in Vectashield containing DAPI (Vector Laboratories). Digital images of metaphases were captured using the Metafer4/MSearch automated metaphase finder system (MetaSystems) equipped with an AxioImager Z2 microscope (Zeiss). After scanning metaphase preparations at 10x magnification, high-resolution images of metaphases were acquired using a Plan-Apochromat 63x/1,40 oil objective.

siRNAs

Target	Sequence
BRCA2	GAAGAAUGCAGGUUUAAUAUU
CHD2-1	GAAACAACCUGCAUAUUUAUU
CHD2-17	GACAAGAACCAUCGCGAUUUU
CHD2-2	CAAGAACCAUCGCGAUUUAUU
CHD2-67	GGGUAAAUGUAGAGAGUGUUU
CHD2-68	GGGUUAAACUCCUGAAGUAUU
CHD2-69	GGGAAAAGGACCAGGGAAAUU
CHD2-70	AGAUUAACGUAGUGGUUUAUU
CHD4	GAGCGGCAGUUCUUUGUGAUU
DNA-PKcs	CUUUAUGGUGGCCAUGGAGUU
H3F3A	GAGAAATTGCTCAGGACTTUU
H3F3B	CAGAGGTTGGTGAGGGAGAUU
KU80	CAAGGAUGAGAUUGCUUUAGU
Luciferase (Luc)	CGUACGCGGAAUACUUCGAUU
PARG (Smart pool)	CCAGUUGGAUGGACACUAA GAUGGUAGUUCCUCCCAAA UACCAGAGCAGUUUAGUAA GGAAACGGUACUCUACUAA
PARP1-1	GAAAGUGUGUUCAACUAAUUU
PARP1-2	AAGAUAGAGCGUGAAGGCGAA
PARP2	AAGGAUUGCUUCAAGGUAAUU
SNF2H	GGAUUAAACUGGCUCAUUUUU
XRCC4	AUAUGUUGGUGAACUGAGAUU

shRNAs

Target	Sequence	TRC number (Sigma Mission Library)
ATM	GTAACATATGACCTCGAAA	
CHD2-a	GCAATATGGACTCTGAGAA	
CHD2-b	GTCTATGATATGCTT	
CHD2-c	GTAACATATGACCTCGAAA	
mouse CHD2-83	CGGATTCGCAGTTCCACTAAA	TRCN0000239016
mouse CHD2-85	TCATCCAGGCAGTACTATTAA	TRCN0000218567
mouse CHD2-87	CAAGAACCATCACGATTTAAT	TRCN0000239015
mouse H3F3A	GCGAGAAATTGCTCAGGACTT	TRCN0000012026
mouse H3F3B-1	GAGATCGCCCAGGATTTCAAA	TRCN0000311286
mouse H3F3B2	GAAGCTGCCATTCCAGAGATT	TRCN0000092921
mouse HIF	GCCCTAGATGGCTTTGTGA	
mouse LigIV	GGATCAGAGACGAGTTACT	
mouse PARP1-08	CCTCTTAGTCTGCTGAGCTTT	TRCN0000071208
mouse PARP1-48	TCGACGTCAACTACGAGAAAC	TRCN0000305948
mouse PARP1-59	GCCCTTGGAAACATGTATGAA	TRCN0000325059
mouse PARP1-959	GAGTACATTGTCTACGACATT	TRCN0000353959
mouse Scr	CAACAAGATGAAGAGCACCAA	

Antibodies

Antibody	Host	Company (reference)	IF	WB
CHD2	Rabbit	Cell signaling (4170)	1:100	1:1000
CHD2	Rat	Millipore (clone 8H3)		1:1000
CHD4	Mouse	Abcam (ab54603)		1:200
DNA-PKcs	Mouse	Abcam (ab1832)		1:500
FLAG	Mouse	Sigma (F 1804)	1:100	
GFP	Mouse	Roche (11814460001)		1:2000
GST	Rabbit	Cell Signaling (2625)		1:1000
H3.3	Rabbit	Millipore Cat.#09-838		1:1000
KU70	Mouse	Santa Cruz (sc-17789)		1:1000
KU80	Rabbit	Santa Cruz (sc-9034)		1:500
LigIV	Rabbit	Novus (#110-57379)		1:800
MDC1	Rabbit	Abcam (ab11171-50)	1:1000	
PAR (10H)	Mouse	Abcam (ab14459)	1:100	
PARP1	Rabbit	Cell Signaling (9542)		1:1000
PARP1	Rabbit	ENZO (ALX-210-302)		1:4000
PARP2	Mouse	ENZO (4G8)		1:200
SNF2H	Rabbit	Abcam (ab3749)		1:1000
tubulin	Mouse	Sigma (T6199)		1:5000
XRCC4	Rabbit	Gift from Dr. M. Modesti	1:500	
γH2AX	Mouse	Millipore (clone JBW301)	1:2000	

Primers

Name	Sequence
CHD2(1-461) FW	GGACTCGGTACCGCCACCATGATGAGAAATAAGGACAAAAG
CHD2(1-461) RV	GAGTCCACCGGTGGCAGGGCCTTGCATTCTCTTG
CHD2(462-951) FW	GGACTCGGTACCGCCACCATGAAGCAGAGACCACGATTTG
CHD2(462-951) RV	GAGTCCACCGGTGGCAGGATCGTCCGGCCAGTG
CHD2(952-1391) FW	GGACTCGGTACCGCCACCATGGAAAACAACTCAGGAAGGTC
CHD2(952-1391) RV	GAGTCCACCGGTGGTTTTTTTTTCATTGGACTTTTTTCCAAGC
CHD2(1392-1828) FW	GGACTCGGTACCGCCACCATGCAGAAGAAGAAAGAGAACAAG
CHD2(1392-1828) RV	GAGTCCACCGGTGGTGTTTTCCGAACATTCCAGTTATAATCTG
CHD2 (1610) RV	GAGTCCACCGGTGGGGCAGGCAAATGAGGCTTC
CHD2 (1611) FW	GGACTCGGTACCGCCACCATGTCCCATGGCCCACAGATGC
CHD2 K515R FW	GATGAAATGGGCCTAGGAGCGACCATCCAGACCATATC
CHD2 K515R RV	GATATGGTCTGGATGGTCGCTCCTAGGCCCATTTCATC

References

Acs, K., M.S. Luijsterburg, L. Ackermann, F.A. Salomons, T. Hoppe, and N.P. Dantuma. 2011. The AAA-ATPase VCP/p97 promotes 53BP1 recruitment by removing L3MBTL1 from DNA double-strand breaks. *Nat Struct Mol Biol*. 18:1345-1350.

Adam, S., S.E. Polo, and G. Almouzni. 2013. Transcription recovery after DNA damage requires chromatin priming by the H3.3 histone chaperone HIRA. *Cell*. 155:94-106.

Bekker-Jensen, S., K. Fugger, J.R. Danielsen, I. Gromova, M. Sehested, J. Celis, J. Bartek, J. Lukas, and N. Mailand. 2007. Human Xip1 (C2orf13) is a novel regulator of cellular responses to DNA strand breaks. *J Biol Chem*. 282:19638-19643.

Bennardo, N., A. Cheng, N. Huang, and J.M. Stark. 2008. Alternative-NHEJ is a mechanistically distinct pathway of mammalian chromosome break repair. *PLoS Genet*. 4:e1000110.

Boersma, V., N. Moatti, S. Segura-Bayona, M.H. Peuscher, J. van der Torre, B.A. Wevers, A. Orthwein, D. Durocher, and J.J. Jacobs. 2015. MAD2L2 controls DNA repair at telomeres and DNA breaks by inhibiting 5' end resection. *Nature*. 521:537-540.

Herce, H.D., W. Deng, J. Helma, H. Leonhardt, and M.C. Cardoso. 2013. Visualization and targeted disruption of protein interactions in living cells. *Nat Commun*. 4:2660.

Ismail, I.H., J.P. Gagne, M.C. Caron, D. McDonald, Z. Xu, J.Y. Masson, G.G. Poirier, and M.J. Hendzel. 2012. CBX4-mediated SUMO modification regulates BMI1 recruitment at sites of DNA damage. *Nucleic Acids Res*. 40:5497-5510.

Janicki, S.M., T. Tsukamoto, S.E. Salghetti, W.P. Tansey, R. Sachidanandam, K.V. Prasanth, T. Ried, Y. Shav-Tal, E. Bertrand, R.H. Singer, and D.L. Spector. 2004. From silencing to gene expression: real-time analysis in single cells. *Cell*. 116:683-698.

Konishi, A., and T. de Lange. 2008. Cell cycle control of telomere protection and NHEJ revealed by a ts mutation in the DNA-binding domain of TRF2. *Genes & development*. 22:1221-1230.

Luijsterburg, M.S., K. Acs, L. Ackermann, W.W. Wiegant, S. Bekker-Jensen, D.H. Larsen, K.K. Khanna, H. van Attikum, N. Mailand, and N.P. Dantuma. 2012a. A new non-catalytic role for ubiquitin ligase RNF8 in unfolding higher-order chromatin structure. *EMBO J*. 31:2511-2527.

Luijsterburg, M.S., M. Lindh, K. Acs, M.G. Vrouwe, A. Pines, H. van Attikum, L.H. Mullenders, and N.P. Dantuma. 2012b. DDB2 promotes chromatin decondensation at UV-induced DNA damage. *J Cell Biol*. 197:267-281.

Mari, P.O., B.I. Florea, S.P. Persengiev, N.S. Verkaik, H.T. Bruggenwirth, M. Modesti, G. Giglia-Mari, K. Bezstarosti, J.A. Demmers, T.M. Luider, A.B. Houtsmuller, and D.C. van Gent. 2006. Dynamic assembly of end-joining complexes requires interaction between Ku70/80 and XRCC4. *Proc Natl Acad Sci U S A*. 103:18597-18602.

Mortusewicz, O., J.C. Ame, V. Schreiber, and H. Leonhardt. 2007. Feedback-regulated poly(ADP-ribosyl)ation by PARP-1 is required for rapid response to DNA damage in living cells. *Nucleic Acids Res*.

Peuscher, M.H., and J.J. Jacobs. 2011. DNA-damage response and repair activities at uncapped telomeres depend on RNF8. *Nat Cell Biol*. 13:1139-1145.

Pierce, A.J., R.D. Johnson, L.H. Thompson, and M. Jasin. 1999. XRCC3 promotes homology-directed repair of DNA damage in mammalian cells. *Genes & development*. 13:2633-2638.

Schimmel, J., K. Eifler, J.O. Sigurethsson, S.A. Cuijpers, I.A. Hendriks, M. Verlaan-de Vries, C.D. Kelstrup, C. Francavilla, R.H. Medema, J.V. Olsen, and A.C. Vertegaal. 2014. Uncovering SUMOylation dynamics during cell-cycle progression reveals FoxM1 as a key mitotic SUMO target protein. *Mol Cell*. 53:1053-1066.

Shah, G.M., F. Kandan-Kulangara, A. Montoni, R.G. Shah, J. Brind'amour, M.D. Vodenicharov, and B. Affar el. 2011. Approaches to detect PARP-1 activation in vivo, in situ, and in vitro. *Methods Mol Biol*. 780:3-34.

Tang, J., N.W. Cho, G. Cui, E.M. Manion, N.M. Shanbhag, M.V. Botuyan, G. Mer, and R.A. Greenberg. 2013. Acetylation limits 53BP1 association with damaged chromatin to promote homologous recombination. *Nat Struct Mol Biol*. 20:317-325.